

## Contribution of under-ice primary production to an ice-edge upwelling phytoplankton bloom in the Canadian Beaufort Sea

C. J. Mundy,<sup>1</sup> Michel Gosselin,<sup>1</sup> Jens Ehn,<sup>2</sup> Yves Gratton,<sup>3</sup> Andrea Rosznagel,<sup>4</sup> David G. Barber,<sup>4</sup> Johannie Martin,<sup>5</sup> Jean-Éric Tremblay,<sup>5</sup> Molly Palmer,<sup>6</sup> Kevin R. Arrigo,<sup>6</sup> Gérald Darnis,<sup>5</sup> Louis Fortier,<sup>5</sup> Brent Else,<sup>4</sup> and Tim Papakyriakou<sup>4</sup>

Received 22 April 2009; revised 21 July 2009; accepted 31 July 2009; published 1 September 2009.

[1] The Canadian Beaufort Sea has been categorized as an oligotrophic system with the potential for enhanced production due to a nutrient-rich intermediate layer of Pacific-origin waters. Using under-ice hydrographic data collected near the ice-edge of a shallow Arctic bay, we documented an ice-edge upwelling event that brought nutrient-rich waters to the surface during June 2008. The event resulted in a 3-week long phytoplankton bloom that produced an estimated  $31 \text{ g C m}^{-2}$  of new production. This value was approximately twice that of previous estimates for annual production in the region, demonstrating the importance of ice-edge upwelling to the local marine ecosystem. Under-ice primary production estimates of up to  $0.31 \text{ g C m}^{-2} \text{ d}^{-1}$  showed that this production was not negligible, contributing up to 22% of the daily averaged production of the ice-edge bloom. It is suggested that under-ice blooms are a widespread yet under-documented phenomenon in polar regions, which could increase in importance with the Arctic's thinning ice cover and subsequent increase in transmitted irradiance to the under-ice environment. **Citation:** Mundy, C. J., et al. (2009), Contribution of under-ice primary production to an ice-edge upwelling phytoplankton bloom in the Canadian Beaufort Sea, *Geophys. Res. Lett.*, 36, L17601, doi:10.1029/2009GL038837.

### 1. Introduction

[2] Arctic sea ice extent has been decreasing throughout the 3-decade satellite record [Comiso et al., 2008]. Rysgaard et al. [1999] found that annual primary production was related to the period of open water and therefore, suggested that Arctic sea ice reduction associated with global warming could enhance primary production. This suggestion was corroborated by Arrigo et al. [2008] who attributed 70% of a  $35 \text{ Tg C yr}^{-1}$  increase in primary production between 2006

and 2007 to an increased phytoplankton growing season in the Arctic Ocean, the remaining 30% attributed to change in geographical extent of the summer minimum sea ice cover. As these results were satellite-derived, conclusions assumed minimal rates of pelagic primary production when areas were ice-covered.

[3] However, phytoplankton have been documented to grow under 100% sea ice cover [e.g., Fukuchi et al., 1989; Gradinger, 1996; Strass and Nöthig, 1996; Fortier et al., 2002; Ichinomiya et al., 2007]. Most of these observations have been made following termination of the spring ice algae bloom and during advanced stages of sea ice melt. Notably, this is a period when sea ice becomes covered by meltponds that greatly increase its transparency to photosynthetically active radiation [Perovich et al., 1998] and stratification of surface waters is strengthened by ice melt [Strass and Nöthig, 1996].

[4] Receding (melting) ice-edges have long been recognized as sites of high biological production potential, but are highly variable in production with respect to time and space [Smith and Nelson, 1986]. The occurrence of wind-induced Ekman upwelling along ice-edges has been shown to bring nutrient-rich waters to the surface and support the development of extensive phytoplankton blooms [Alexander and Niebauer, 1981]. In the coastal Beaufort Sea, low salinity (<31.6) nutrient-poor polar surface water (PSW) is underlain by an intermediate layer (32.4–33.1 core salinity; <−1°C; ~250 m maximum depth) of relatively nutrient-rich (maximum values of ~15, 2 and 30 mmol m<sup>−3</sup> for nitrate, phosphate and silicate, respectively) Pacific-origin waters (IPW) [Carmack et al., 2004]. IPW has been noted to be of great importance to the Beaufort Sea for its potential to enhance biological production where it mixes into PSW [Carmack et al., 2004]. Tremblay et al. [2008] showed that a lack of winter mixing limited primary production in the region by hindering injection of nutrients from IPW into surface waters, however an isolated eddy-like feature was noted to bring IPW to the surface. Furthermore, wind-induced Ekman upwelling of IPW to the surface has been observed to occur along the Canadian Beaufort Shelf [Williams and Carmack, 2008].

[5] Considering recent observations of enhanced open ocean primary production in the Arctic Ocean due to the reduction of sea ice cover [Arrigo et al., 2008], it is important to determine the role that under-ice primary production plays in polar regions. However, under-ice production has not been extensively documented, mainly due to logistical difficulties of collecting data during late stages of sea ice melt. During the International Polar Year – Circumpolar Flaw Lead

<sup>1</sup>Institut des Sciences de la Mer, Université du Québec à Rimouski, Rimouski, Québec, Canada.

<sup>2</sup>Laboratoire d'Océanographie de Villefranche, Université Pierre et Marie Curie-Paris VI, CNRS, Villefranche-sur-Mer, France.

<sup>3</sup>Institut National de la Recherche Scientifique—Eau, Terre et Environnement, Université du Québec, Québec, Québec, Canada.

<sup>4</sup>Centre for Earth Observation Science, Faculty of Environment, Earth and Resources, University of Manitoba, Winnipeg, Manitoba, Canada.

<sup>5</sup>Québec-Océan, Département de biologie, Université Laval, Québec, Québec, Canada.

<sup>6</sup>Department of Environmental Earth System Science, Stanford University, Stanford, California, USA.

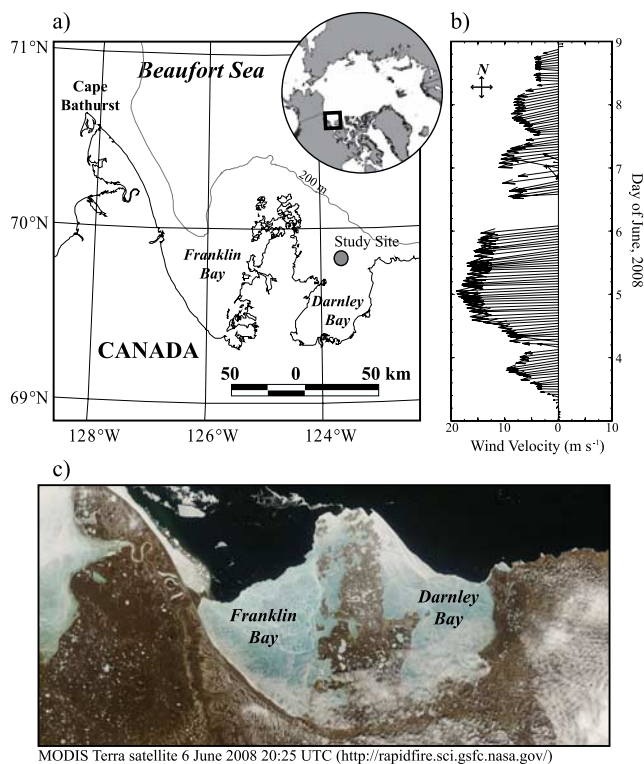


**Figure 1.** (a) Map of study location in Darnley Bay, NT, Canada. (b) A feather plot of hourly averaged wind vectors obtained from the meteorological tower on the CCGS *Amundsen* and (c) an image of the landfast ice-edge in Darnley Bay obtained from the Moderate Resolution Imaging Spectroradiometer (MODIS) aboard NASA's Terra satellite.

system study (IPY-CFL 2008 (D. G. Barber et al., The International Polar Year (IPY) Circumpolar Flaw Lead (CFL) system study: Introduction and physical system, submitted to *Atmosphere-Ocean*, 2009)), we documented an ice-edge upwelling event that brought IPW to the surface. The event resulted in an enhanced 3-week long phytoplankton bloom. As our observations were made under the landfast ice approximately 1 km from the ice-edge in Darnley Bay, the data provided unique insights into the contribution of under-ice primary production to the ice-edge bloom.

## 2. Data Set

[6] Data presented were collected onboard the Canadian Coast Guard Ice Breaker CCGS *Amundsen* between 3–24 June 2008. Wind speed and direction were obtained using an RM-Young anemometer, mounted ~14 m from the water surface on a tower at the bow of the ship. Downwelling incident photosynthetically active radiation (PAR; 400–700 nm) also was monitored on the ship. Hydrographic data prior to 24 June were collected under a landfast first-year sea ice cover in Darnley Bay, Canadian Beaufort Sea (69°49.6'N, 123°37.9'W, water depth ~80 m; Figure 1a) via both the ship's moonpool and a hole in the sea ice made ~500 m from the ship. On 24 June, data were collected in open water 2-days after the ice had broken up in Darnley Bay. Profiles of temperature, salinity and *in vivo* chlorophyll *a* (chl *a*) and nitrate concentration from

10 to 65 m were measured with a rosette mounted SBE-911 plus CTD sensor (Sea-Bird Electronics, Inc.), equipped with a fluorometer (Seapoints Sensors, Inc.) and nitrate sensor (Satlantic). As described by Tremblay et al. [2008], a quadratic polynomial was used to calibrate fluorometer data against extracted chl *a* measurements [Parsons et al., 1984] from discrete water samples ( $n = 38$ ;  $r^2 = 0.94$ ). Colorimetrically determined nitrate concentrations from water samples (following Tremblay et al. [2008]) were used to calibrate the nitrate sensor data using a linear regression ( $n = 29$ ,  $r^2 = 0.87$ ). A re-calibration of the nitrate sensor was made following re-deployment of the instrument on 22 June ( $n = 7$ ,  $r^2 = 0.94$ ). Above 10 m, water samples collected using either a Kemmerer water sampler or electric submersible pump through the ice hole were used to measure surface chl *a* and nitrate concentrations, completing the profiles up to the bottom of the sea ice. Particulate organic carbon (POC) was measured on water subsamples filtered through pre-combusted (450°C) GF/F filters dried at 60°C for 24 h and analyzed using a Costech ECS 4010 CHN analyzer. Vertical net tows (200  $\mu\text{m}$  mesh) were used to estimate mesozooplankton abundance integrated over the water column. During the study, photosynthesis-irradiance (P-I) curves were estimated on 12 and 18 June from water samples at the depth of the chl *a* maximum using a photosynthetron and <sup>14</sup>C as a tracer following Lewis and Smith [1983]. Under-ice PAR profiles were obtained via a free-falling optical radiometer (Satlantic HyperOCR) with surface reference and deployed with the aid of SCUBA divers directly under the ice cover approximately 25 m from the ice hole. On 24 June in open water, a PAR radiometer (Biospherical Instruments Inc.) mounted to the rosette with surface reference was used to obtain the light profile.

## 3. Ice-Edge Upwelling Bloom

[7] At the start of the study period, sustained easterly winds of  $>10 \text{ m s}^{-1}$  were observed over a 72 h period (4 to 7 June; Figure 1b). Winds of  $10 \text{ m s}^{-1}$  equate to a surface wind stress of  $0.17 \text{ N m}^{-2}$ . At the latitude of our study, the inertial period ( $T = 2\pi/f$ , where  $f$  is the Coriolis parameter) is ~12.8 h. Therefore, with the observed winds exerting a sustained wind stress of  $0.17 \text{ N m}^{-2}$  over several inertial periods, the time scale was ample to develop the observed ice-edge upwelling event (Figures 2a–2c). Modeling work on upwelling at landfast ice-edges have suggested that the horizontal size structure is equal to two times the Rossby radius of deformation ( $R_i$ ) [Clarke, 1978]. Therefore, using the water column structure observed prior to the upwelling event, we calculated a  $R_i$  of ~3.3 km and estimated the horizontal scale of the upwelling event to be ~6.6 km.

[8] Figures 2a–2c show the upwelling event that occurred between our hydrographic profiles taken on 4 and 7 June. The 32.5 salinity isoline demonstrated that water from approximately 40 m was transported to the upper 10 m of the water column during the event, which equated to an upwelling velocity of  $8.3 \text{ m d}^{-1}$ . This velocity was very close to that estimated by Alexander and Niebauer [1981] for a mobile ice edge under similar atmospheric forcing conditions. The 32.5 salinity isoline was within the range of the IPW core salinity showing that these waters were transported to the surface where phytoplankton were

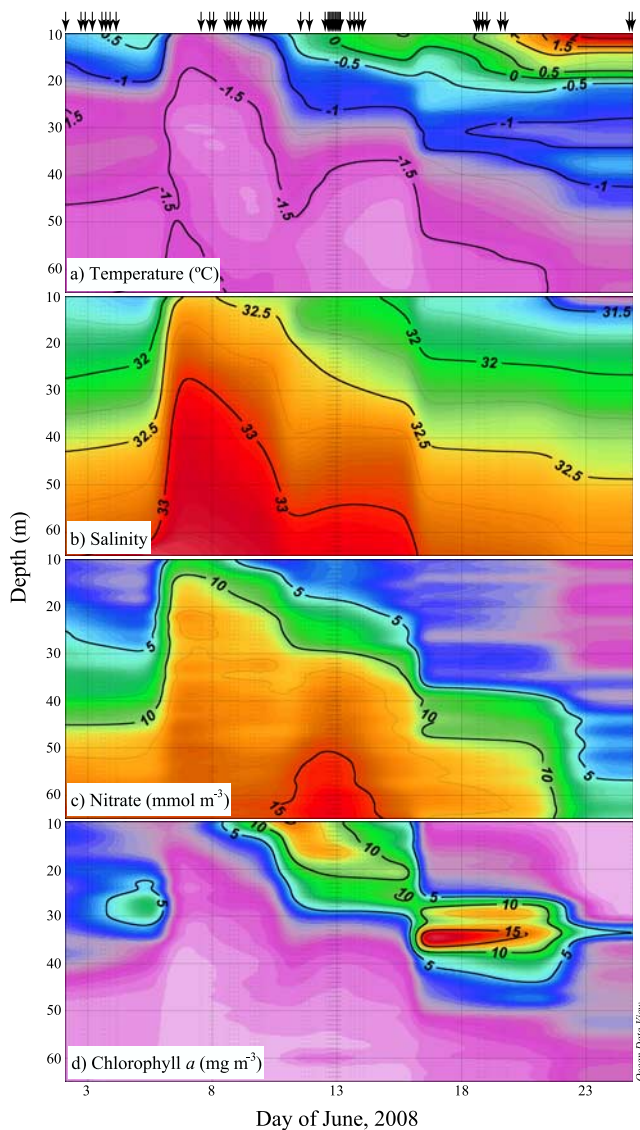


**Figure 2.** Interpolated time series of (a) temperature, (b) salinity, (c) nitrate concentration and (d) chl *a* concentration (via *in vivo* fluorescence) observed at the Darnley Bay sampling station. Major (labeled) and minor isolines were plotted at regular intervals. Data from 47 hydrocasts (arrows) were interpolated and plotted using Ocean Data View v. 3.3.1 [Schlitzer, 2006].

able to make use of the nutrient-rich waters within the euphotic zone. Chl *a* biomass accumulated just above the 32.5 salinity isoline along the nutricline, which steadily dropped as the water column settled following the upwelling event (Figures 2b–2d). The depletion of nitrate was evident above the descending bloom. Chl *a* accumulation reached peak values of 25 mg m<sup>-3</sup> and 345 mg m<sup>-2</sup> integrated over the upper 50 m of the water column. These concentrations significantly exceeded the maximum chl *a* concentrations of 2.5 mg m<sup>-3</sup> and 55 mg m<sup>-2</sup>, respectively, observed in Franklin Bay (adjacent to Darnley Bay) during the annual study of Tremblay *et al.* [2008] in 2003–2004.

[9] As described by Riedel *et al.* [2008], the accumulation of biomass integrated over the upper 50 m of the water

column from 7 to 12 June was used to estimate the net accumulation rate of phytoplankton biomass. The slope from an exponential curve fit to the time series data provided a specific accumulation rate of 0.43 d<sup>-1</sup> ( $n = 19$ ,  $r^2 = 0.95$ ; see S1 of the auxiliary material).<sup>1</sup> Applying the measured POC:chl *a* ratio of 42.8 (g:g), and multiplying the specific accumulation rate by the average biomass over the time period, we estimated a net accumulation rate of 2.8 g C m<sup>-2</sup> d<sup>-1</sup>. Following 12 June, chl *a* concentrations integrated over the upper 50 m of the water column varied between 150 and 350 mg m<sup>-2</sup>, then decreased to 41 mg m<sup>-2</sup> by the end of the period, suggesting that losses due to grazing and/or sinking of phytoplankton rapidly superceded primary production as the nutricline descended.

[10] During our study, mesozooplankton abundance integrated over the water column (80 m depth) averaged ( $\pm$ SD)  $23 \times 10^3$  ( $16 \times 10^3$ ) ind. m<sup>-2</sup>, which was similar to previous observations made for the same time of year [Forest *et al.*, 2008]. Forest *et al.* [2008] observed minimal interception of the spring phytoplankton bloom by mesozooplankton. Similarly, it is likely that little of the ice-edge bloom was grazed by mesozooplankton during our study. In fact, mesozooplankton abundance decreased over the bloom period. Microzooplankton abundance and activity were not measured during this study. However, low water temperatures observed during our study ( $<0^\circ\text{C}$ ) likely reduced consumption of phytoplankton by micrograzers, as recently shown in the western Arctic Ocean by Sherr *et al.* [2009].

[11] Removal of nitrate from the water column was used to estimate new primary production following Smith *et al.* [1991]. Salinity profiles measured immediately before the upwelling event and after the phytoplankton bloom, on 2 and 24 June, respectively, were identical, suggesting similar water masses, while nitrate concentrations measured from discrete water samples were much less on 24 June. Applying the C:N molar ratio of 7.3 observed for the region [Tremblay *et al.*, 2008], the reduction in nitrate concentration between 2 and 24 June integrated over the water column equated to a new primary production estimate of 31 g C m<sup>-2</sup> and a daily averaged rate of 1.4 g C m<sup>-2</sup> d<sup>-1</sup>. Previous annual production estimates for the Beaufort Sea have ranged from 10 to 15 g C m<sup>-2</sup> a<sup>-1</sup> [Alexander, 1974; Carmack *et al.*, 2004; Tremblay *et al.*, 2008], which has historically led to classification of the Beaufort Sea as oligotrophic. Our primary production estimates over a 3-week period exceed these previous values by a factor of two. This difference demonstrates the importance of ice-edge upwelling events to local primary production, particularly in the Beaufort Sea where surface waters overlay nutrient-rich IPW.

#### 4. Under-Ice Primary Production

[12] The close proximity of our under-ice sampling site to the ice-edge ( $<1$  km) and an estimate of the horizontal scale of upwelling circulation of  $\sim 6.6$  km, suggested that at least a portion of the under-ice phytoplankton biomass was advected from the open water region. To estimate the contribution of under-ice primary production to total production in the region, we used P-I curves combined with

<sup>1</sup>Auxiliary materials are available in the HTML. doi:10.1029/2009GL038837.

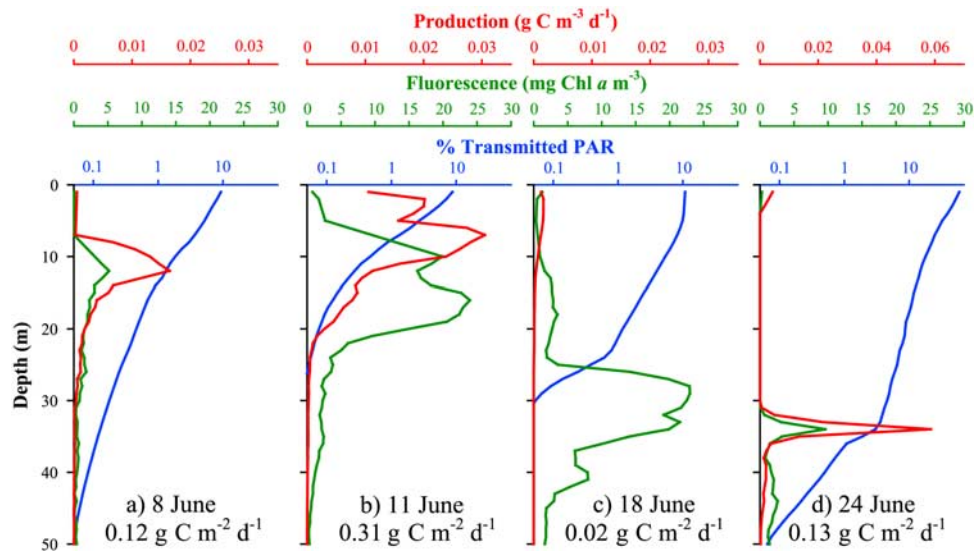


**Figure 3.** (a–c) Under-ice and (d) open water daily primary production estimates calculated using profiles of chl *a* concentration (via *in vivo* fluorescence) and percent transmitted PAR, and photosynthesis versus irradiance relationships (P-I curves) measured from water samples. Values reported at the bottom of each plot represent the integrated production over the upper 50 m of the water column. Note the change in scale for the 24 June primary production plot. Profiles start at the bottom of the sea ice cover (depth from water surface; Figures 3a–3c) and at 1 m in the open water (Figure 3d).

under-ice light profiles, downwelling surface PAR and chl *a* concentration profiles following Carmack *et al.* [2004], using the P-I equation of Platt *et al.* [1980]:

$$\int_t \int_z \left( \left( P_s^B \left( 1 - e^{-\alpha^B I_{z,t}/P_s^B} \right) e^{-\beta^B I_{z,t}/P_s^B} \right) [chl a]_z \right) dz dt, \quad (1)$$

where  $P_s^B$  is the chl *a*-normalized maximum photosynthetic rate if there were no photoinhibition ( $\text{mg C mg chl } a^{-1} \text{ h}^{-1}$ ),  $\alpha^B$  is the photosynthetic efficiency ( $\text{mg C mg chl } a^{-1} \text{ h}^{-1} (\mu\text{mol photons m}^{-2} \text{ s}^{-1})^{-1}$ ),  $\beta^B$  is the photoinhibition parameter (same units as  $\alpha^B$ ),  $I_{z,t}$  is the transmitted irradiance at depth  $z$  and time  $t$  ( $\mu\text{mol photons m}^{-2} \text{ s}^{-1}$ ) and  $[chl a]_z$  is the chl *a* concentration at depth  $z$  ( $\text{mg chl } a \text{ m}^{-3}$ ). Figure 3 shows daily integrated primary production for under-ice profiles on 8, 11 and 18 June and for an open water profile on 24 June.

[13] Approximately 10% of surface PAR penetrated the 1 to 1.5 m-thick sea ice cover to a 2 m water depth compared with 52% penetrating the surface ocean on 24 June. Under-ice transmitted irradiances of 0.1% of surface PAR reached depths up to 37 m depending on water column attenuation properties, which were influenced greatly by phytoplankton biomass. Under-ice primary production integrated over the upper 50 m of the water column ranged from 0.02 to 0.31  $\text{g C m}^{-2} \text{ d}^{-1}$ . Therefore, under-ice primary production contributed up to 22% of the daily averaged ice-edge bloom production of 1.4  $\text{g C m}^{-2} \text{ d}^{-1}$ . It is noted that ice algae chl *a* concentration monitored in the bottom 10 cm of the ice cover remained  $<0.5 \text{ mg chl } a \text{ m}^{-2}$  throughout the study period.

[14] The key to the high under-ice production observed in our study was having high biomass and nutrients near the surface where phytoplankton had access to sufficient transmitted irradiance under the ice cover. These conditions represent perhaps a special case, where ice-edge upwelling of nutrients and advected phytoplankton biomass produced

in the adjacent open water region augmented the primary production capacity under the ice cover. Therefore, our estimates may represent the upper bound to under-ice production in the Arctic. However, other regions, such as the Canadian Arctic Archipelago, also may provide exceptional pre-conditioning for the development of an under ice bloom. That is, high surface nutrients, a function of mixing of IPW in the shallow and narrow waterways of the Archipelago [Michel *et al.*, 2006], and a landfast first-year ice cover, provide the potential for a late season under-ice phytoplankton bloom. Supporting this statement was the observation of greater than 450  $\text{mg m}^{-2}$  pelagic chl *a* concentrations in the under-ice water column in Resolute Passage [Fortier *et al.*, 2002]. Furthermore, during springtime, the under-ice water column of the Arctic, and polar regions in general, can become relatively nutrient-rich due to winter mixing processes and seasonal darkness. The positive-feedback processes of snow melt and meltpond formation at the ice surface result in a rapid increase in the average euphotic zone irradiance that, when combined with meltwater input which influences surface stratification, provide the perfect conditions for a bloom. Therefore, we suggest that under-ice phytoplankton blooms are a widespread, yet, under documented phenomenon in polar regions.

## 5. Conclusions

[15] It was previously noted that only a handful of studies exist on the subject of under-ice phytoplankton. Most of these investigations, in addition to the data presented in the current study, have demonstrated that under-ice primary production is not trivial. However, the lack of information makes it currently unreasonable to provide an estimate of the under-ice contribution to total polar primary production. Future work is warranted on the subject to better understand the dynamics of polar marine ecosystems and their response to the rapidly changing climate. This statement is particu-

larly relevant provided the observations and model predictions of a thinning Arctic ice cover [Lindsay and Zhang, 2005], which will provide an increasing amount of transmitted irradiance to the late season under-ice pelagic environment.

[16] **Acknowledgments.** This work is a contribution to the International Polar Year-Circumpolar Flaw Lead system study (IPY-CFL 2008), supported through grants from the Canadian IPY Federal program office, the Natural Sciences and Engineering Research Council and numerous international collaborators. We would like to extend our gratitude to the SCUBA divers, J. Stewart and H. Hop and to D. Leitch, B. Philippe, P. Guillot, S. Blondeau, V. Lago, S. Dyck, C. Brouard, S. Pineault, L. Létourneau, M. Ringuette, S. Thanassekos, H. Cloutier, S. Lauzon and the officers and crew of the CCGS *Amundsen* for logistical and post-processing support.

## References

- Alexander, V. (1974), Primary production regimes of the nearshore Beaufort Sea, with reference to potential roles of ice biota, in *The Coast and Shelf of the Beaufort Sea*, edited by J. C. Reed and J. E. Sater, pp. 609–632, Arct. Inst. of North America, Arlington, Va.
- Alexander, V., and H. J. Niebauer (1981), Oceanography of the eastern Bering Sea ice-edge zone in spring, *Limnol. Oceanogr.*, *26*, 1111–1125.
- Arrigo, K. R., G. van Dijken, and S. Pabi (2008), Impact of a shrinking Arctic ice cover on marine primary production, *Geophys. Res. Lett.*, *35*, L19603, doi:10.1029/2008GL035028.
- Carmack, E. C., R. W. Macdonald, and S. Jasper (2004), Phytoplankton productivity on the Canadian Shelf of the Beaufort Sea, *Mar. Ecol. Prog. Ser.*, *277*, 37–50, doi:10.3354/meps277037.
- Clarke, A. J. (1978), On wind-driven quasi-geostrophic water movements near fast ice edges, *Deep Sea Res.*, *25*, 41–51.
- Comiso, J. C., C. L. Parkinson, R. Gersten, and L. Stock (2008), Accelerated decline in the Arctic sea ice cover, *Geophys. Res. Lett.*, *35*, L01703, doi:10.1029/2007GL031972.
- Forest, A., M. Sampei, R. Makabe, H. Sasaki, D. G. Barber, Y. Gratton, P. Wassmann, and L. Fortier (2008), The annual cycle of particulate organic carbon export in Franklin Bay (Canadian Arctic): Environmental control and food web implications, *J. Geophys. Res.*, *113*, C03S05, doi:10.1029/2007JC004262.
- Fortier, M., L. Fortier, C. Michel, and L. Legendre (2002), Climatic and biological forcing of the vertical flux of biogenic particles under seasonal Arctic sea ice, *Mar. Ecol. Prog. Ser.*, *225*, 1–16, doi:10.3354/meps225001.
- Fukuchi, M., K. Watanabe, A. Tanimura, T. Hoshiai, H. Sasaki, H. Satoh, and Y. Yamaguchi (1989), A phytoplankton bloom under sea ice recorded with a moored system in Lagoon Saroma Ko, Hokkaido, Japan, *Proc. NIPR Symp. Polar Biol.*, *2*, 9–15.
- Gradinger, R. (1996), Occurrence of an algal bloom under Arctic pack ice, *Mar. Ecol. Prog. Ser.*, *131*, 301–305, doi:10.3354/meps131301.
- Ichinomiya, M., M. Honda, H. Shimoda, K. Saito, T. Odate, M. Fukuchi, and A. Taniguchi (2007), Structure of the summer under fast ice microbial community near Syowa Station, eastern Antarctica, *Polar Biol.*, *30*, 1285–1293, doi:10.1007/s00300-007-0289-8.
- Lewis, M. R., and J. C. Smith (1983), A small volume, short-incubation-time method for measurement of photosynthesis as a function of incident irradiance, *Mar. Ecol. Prog. Ser.*, *13*, 99–102, doi:10.3354/meps013099.
- Lindsay, R. W., and J. Zhang (2005), The thinning of Arctic sea ice, 1988–2003: Have we passed a tipping point?, *J. Clim.*, *18*, 4879–4894, doi:10.1175/JCLI3587.1.
- Michel, C., R. G. Ingram, and L. R. Harris (2006), Variability in oceanographic and ecological processes in the Canadian Arctic Archipelago, *Prog. Oceanogr.*, *71*, 379–401, doi:10.1016/j.pocean.2006.09.006.
- Parsons, T. R., Y. Maita, and C. M. Lalli (1984), *A Manual of Chemical and Biological Methods for Seawater Analysis*, 173 pp., Pergamon, New York.
- Perovich, D. K., C. S. Roesler, and W. S. Pegau (1998), Variability in Arctic sea ice optical properties, *J. Geophys. Res.*, *103*, 1193–1208, doi:10.1029/97JC01614.
- Platt, T., C. L. Gallegos, and W. G. Harrison (1980), Photoinhibition of photosynthesis in natural assemblages of marine phytoplankton, *J. Mar. Res.*, *38*, 687–701.
- Riedel, A., C. Michel, M. Gosselin, and B. LeBlanc (2008), Winter-spring dynamics in sea-ice carbon cycling in the coastal Arctic Ocean, *J. Mar. Syst.*, *74*, 918–923, doi:10.1016/j.jmarsys.2008.01.003.
- Rysgaard, S., T. G. Nielsen, and B. W. Hansen (1999), Seasonal variation in nutrients, pelagic primary production and grazing in a high-Arctic coastal marine ecosystem, Young Sound, Northeast Greenland, *Mar. Ecol. Prog. Ser.*, *179*, 13–25, doi:10.3354/meps179013.
- Schlitzer, R. (2006), Ocean Data View, <http://odv.awi.de>, Alfred Wegener Inst. for Polar and Mar. Res., Bremerhaven, Germany.
- Sherr, E. B., B. F. Sherr, and A. J. Hartz (2009), Microzooplankton grazing impact in the western Arctic Ocean, *Deep Sea Res., Part II*, *56*, 1264–1273, doi:10.1016/j.dsr2.2008.10.036.
- Smith, W. O., Jr., and D. M. Nelson (1986), Importance of ice edge phytoplankton production in the Southern Ocean, *BioScience*, *36*, 251–257, doi:10.2307/1310215.
- Smith, W. O., Jr., L. A. Codispoti, D. M. Nelson, T. Manley, E. J. Buskey, H. J. Niebauer, and G. F. Cota (1991), Importance of *Phaeocystis* blooms in the high-latitude ocean carbon cycle, *Nature*, *352*, 514–516, doi:10.1038/352514a0.
- Strass, V. H., and E.-M. Nöthig (1996), Seasonal shifts in ice edge phytoplankton blooms in the Barents Sea related to the water column stability, *Polar Biol.*, *16*, 409–422, doi:10.1007/BF02390423.
- Tremblay, J.-É., K. Simpson, J. Martin, L. Miller, Y. Gratton, D. Barber, and N. M. Price (2008), Vertical stability and the annual dynamics of nutrients and chlorophyll fluorescence in the coastal, southeast Beaufort Sea, *J. Geophys. Res.*, *113*, C07S90, doi:10.1029/2007JC004547.
- Williams, W. J., and E. C. Carmack (2008), Combined effect of wind-forcing and isobath divergence on upwelling at Cape Bathurst, Beaufort Sea, *J. Mar. Res.*, *66*, 645–663, doi:10.1357/002224008787536808.
- K. R. Arrigo and M. Palmer, Department of Environmental Earth System Science, Stanford University, Stanford, CA 94305, USA.
- D. G. Barber, B. Else, T. Papakyriakou, and A. Rossnagel, Centre for Earth Observation Science, Faculty of Environment, Earth and Resources, University of Manitoba, 125 Drysdale Road, Winnipeg, MB R3T 2N2, Canada.
- G. Darnis, L. Fortier, J. Martin, and J.-É. Tremblay, Québec-Océan, Département de biologie, Université Laval, Pavillon Alexandre-Vachon, 2079-A, Québec, QC G1V 0A6, Canada.
- J. Ehn, Laboratoire d'Océanographie de Villefranche, Université Pierre et Marie Curie-Paris VI, CNRS, F-06238 Villefranche-sur-Mer CEDEX, France.
- M. Gosselin and C. J. Mundy, Institut des Sciences de la Mer, Université du Québec à Rimouski, 310, allée des Ursulines, Rimouski, QC G5L 3A1, Canada. (christopher-john.mundy@uqar.qc.ca)
- Y. Gratton, Institut National de la Recherche Scientifique—Eau, Terre et Environnement, Université du Québec, 490 de la Couronne, Québec, QC G1K 9A9, Canada.